State Estimation of Nonlinear Differential-Algebraic Models of Power Networks with Solar Farms and Dynamic Loads

Muhammad Nadeem and Ahmad F. Taha

***Abstract*— State-of-the-art state estimation routines of electrical grids are reliant on dynamic models of fossil fuel-based resources. These models commonly contain differential equations describing synchronous generator models and algebraic equations modeling power flow/balance equations. Fuel-free power systems that are driven by inertia-less renewable energy resources will hence require new models and upgraded estimation routines. In this paper, we propose a robust estimator for an interconnected model of power networks comprised of a comprehensive ninth order synchronous generator model, advanced power electronics-based models for photovoltaic (PV) power plants, constant power loads, constant impedance loads, and motor loads. The presented state estimator design is based on Lyapunov stability criteria for nonlinear differential algebraic equation (DAE) models and is posed as a convex semi-definite optimization problem. Thorough simulations studies have been carried out on IEEE 39-bus test system to showcase the robustness of the proposed estimator against unknown uncertainty from load demand and solar irradiance.**

I. Introduction and Paper Contributions

POWER systems are moving rapidly toward a greener and more sustainable future through the widespread installation of renewable energy resources (RERs). The intermittent and volatile nature of RERs has created challenges in modern power systems and made the secure and reliable operation of the grid more difficult. To gain network-wide observability of systems with large penetration of renewables, dynamic state estimation (DSE) for the next generation of smart power grids will be essential to perform realtime frequency and voltage regulation. In particular DSE can provide accurate estimates of the physical states of electrical grid which can be highly beneficial for the realtime feedback control and health monitoring of renewables-heavy grids [1].

In this regard, thorough research has been carried out in the past two decades in power system DSE mainly focusing on estimating generator internal states (rotor angle and frequency) and algebraic states (voltage and current phasors). All of the current DSE algorithms can be divided into two broad categories: *(i)* deterministic observers and *(ii)* Kalman filters, its variants, and other statistical and stochastic estimation algorithms. In deterministic observers the basic idea is as follows: First, a dynamical model for the error dynamics is computed (this model explains the evolution of error between original and estimated state variables), then an observer gain is designed based on Lyapunov stability notions. For example, [2] proposed L_∞ based observer design for a two-axis fourth-order synchronous generator model while considering nonlinearities as Lipschitz continuous. However, the algebraic constraint (power flow/balance equations) related to the power network has been neglected. This study has been improved later on in [3] and generator power flow/balance equations have been modeled while performing DSE, however a linear power system model has been considered, which is not realistic as power systems never really operate linearly and are highly nonlinear systems because of the stochastic nature of generation and demand [4]. In [5] a multiplier based observer has been proposed for a nonlinear DAE model of power system, however a simplified synchronous generator model (modeling generator rotor angle only) has been used while performing DSE. Similarly in [6] a 2^{nd} order sliding mode observer for a nonlinear DAE model of power system has been proposed. However, a linearized and simplified generator model has been used and also the reactive power balance equations have been neglected.

On the other hand Kalman filters (KF) are iterative algorithms that require repetitive change of gain matrices while exploiting statistical properties (such as normal distribution) of the noise/disturbances. Such as in [7] researchers have proposed an extended Kalman filter (EKF) for a nonlinear DAE model of power system. Since EKF cannot handle unknown inputs and non-Gaussian process/measurement noise, H_∞ based EKF (HEKF) and extended EKF (EKF-UI) have been proposed in [8], [9]. Moreover, since EKF linearizes the nonlinearities around a certain equilibrium point, thus to avoid linearization, unscented Kalman filter (UKF) and extended particle filter (EPF) have been proposed in [10], [11].

A thorough summary of the techniques used for power system DSE can be found in this recent survey paper [1], while a thorough comparative study between different derivatives of Kalman filter can be found in [12]. Similarly, a comparative analysis between Kalman filters and deterministic observers is presented in [13].

In the aforementioned literature, DSE algorithms are based on a simple power system model capturing only dynamical model of synchronous generators. Thus, the monitoring scope of DSE is mainly limited to the estimation of generator internal states and subsequently algebraic states. However, with the rapid deployment of solar PV power plants and dynamic loads, traditional power systems models are gradually becoming less representative of the dynamics [1]. To achieve grid-wise situational awareness in the future power

This work is supported by National Science Foundation under grants 2013739 and 2151571.

The authors are with the Civil and Environmental Engineering Department, Vanderbilt University, 2201 West End Ave, Nashville, Tennessee 37235. muhammad.nadeem@vanderbilt.edu, ahmad.taha@vanderbilt.edu

systems, it is hence important to model solar PV power plants and dynamic loads with advanced synchronous generator models and algebraic power constraints. This would result in a representative model of power models via a large-scale, nonlinear DAE model to be used for performing DSE.

Key literature gap. Unfortunately, the literature on state estimation of multi-machine power network models with synchronous machines, solar PV power plants, and motor loads (or a combination of these three) while considering PMU measurements models and algebraic constraints is virtually non-existent. In the recent study [14] DSE has been extended and state estimation for a detailed PV power plant model has been reported. However, the study is limited to distribution network only and does not estimate algebraic variables and synchronous generators' internal states. To the best of the authors' knowledge, this paper is the first study that considers DSE of power networks comprised of traditional generators, solar farms, and motor loads while still considering algebraic power/current balance constraints.

Paper Contributions. The paper's contributions are:

- We present a simple DSE method for an advanced model of a power system having ninth-order synchronous generator model, power electronics-based models of solar farms, motor loads, constant power and impedance loads. The proposed DSE algorithm can simultaneously estimate all the states of the power system that include dynamic states of solar farm, loads and algebraic states. To the best of the authors' knowledge, this contribution is the first of its kind in the power systems literature.
- To design an estimator that can handle load fluctuations and uncertainty from RERs, we propose an H_∞-based state estimation technique. The advantage of H_∞-based state estimator over statistical methods is that no prior knowledge of the uncertainty statistics is required and the observer gain is time-invariant.
- We showcase the performance of the proposed estimator on Case 39 power system which is widely used for DSE studies in power systems.

The rest of the paper is organized as follows: Section II summarizes the solar and load integrated DAE model of power systems; Section III discuses the proposed estimator design; Section IV showcases simulation studies and the paper is concluded in Section V.

Notation. The notations $\boldsymbol{O}$ and $\boldsymbol{I}$ denotes the zero and identity matrix of appropriate dimensions respectively. The notation $\mathbb{R}^n$ represent a set of row vector with n elements. Similarly $\mathbb{R}^{m\times n}$ represent a real matrix of size m-by-n. The set of symmetric n-by$n$ matrices are denoted by $\mathbb{S}^n$ and $\mathbb{S}^n_+$ denotes the set of positive semidefinite matrices. The operators $\mathrm{Diag}(\cdot)$ create a diagonal matrix while the symbol $*$ denotes symmetric entries in a symmetric matrix.

II. Solar and Load Integrated DAE Model

We consider a graphical model of the electrical grid with N number of buses, $\mathcal{N} = \{1, ..., N\}$ set of nodes and $\mathcal{E} \subseteq \mathcal{N} \times \mathcal{N}$ set of transmission lines. The overall power system is assumed to have: G number of synchronous machines, R number of PV power plants, and L_p, L_z and K number of constant power, constant impedance, and motor loads respectively. Notice that $\mathcal{N} = \mathcal{G} \cup \mathcal{R} \cup \mathcal{L}$, where $\mathcal{G}, \mathcal{R}$ and $\mathcal{L}$ denotes a set of buses containing synchronous machines, renewables, and loads respectively. To that end, we model the solars- and loads-integrated synchronous machines-DAE (**SLS-DAE**) model of power systems using a set of differential-algebraic equations as follows:

$$\textit{system dynamics:} \quad \dot{\boldsymbol{x}}(t) = \boldsymbol{f}(\boldsymbol{x}_d, \boldsymbol{x}_a, \boldsymbol{u}, \boldsymbol{w}) \tag{1a}$$

$$\textit{algebraic constraints:} \quad \boldsymbol{0} = \boldsymbol{h}(\boldsymbol{x}_d, \boldsymbol{x}_a, \boldsymbol{u}, \boldsymbol{w}) \tag{1b}$$

where $\boldsymbol{x}_d \in \mathbb{R}^{n_d}$ denotes differential variables, $\boldsymbol{x}_a \in \mathbb{R}^{n_a}$ denotes algebraic variables, $\boldsymbol{w} \in \mathbb{R}^{n_w}$ models the exogenous disturbances to the system, and $\boldsymbol{u} \in \mathbb{R}^{n_u}$ models a set of commands that are used to drive the grid to a desirable state. In (1) we model $\boldsymbol{x}_a$ as:

$$\boldsymbol{x}_a(t) := \boldsymbol{x}_a = \begin{bmatrix} \boldsymbol{V}_{Re}^\top & \boldsymbol{V}_{Im}^\top & \boldsymbol{I}_{Re}^\top & \boldsymbol{I}_{Im}^\top \end{bmatrix}^\top \tag{2}$$

where $\boldsymbol{V}_{Re} = \{V_{Re_i}\}_{i\in\mathcal{N}}, \boldsymbol{V}_{Im} = \{V_{Im_i}\}_{i\in\mathcal{N}}, \boldsymbol{I}_{Re} = \{I_{Re_i}\}_{i\in\mathcal{N}}$ and $\boldsymbol{I}_{Im}=\{I_{Im_i}\}_{i\in\mathcal{N}}$ denotes the real and imaginary part of voltage and current phasors respectively. The vector $\boldsymbol{u}$ contains reference inputs to the generators and PV plant and is modeled as: $\boldsymbol{u} = \begin{bmatrix} \boldsymbol{u}_G^\top & \boldsymbol{u}_R^\top \end{bmatrix}^\top$ where $\boldsymbol{u}_G$ contains voltage reference set points $\boldsymbol{V}_{\text{ref}}$ and steam/hydro valve reference positions $\boldsymbol{P}_{v_{\text{ref}}}$ for the synchronous machines, such that $\boldsymbol{u}_G = \begin{bmatrix} \boldsymbol{V}_{\text{ref}}^\top & \boldsymbol{P}_{v_{\text{ref}}}^\top \end{bmatrix}$. Similarly $\boldsymbol{u}_R = \begin{bmatrix} \boldsymbol{V}_{\text{ref}}^\top & \boldsymbol{P}_{\text{ref}}^\top \end{bmatrix}$, where $\boldsymbol{V}_{\text{ref}}$ is the voltage reference and $\boldsymbol{P}_{\text{ref}}$ is the power reference set points for PV power plants. Similarly, vector $\boldsymbol{w}$ in (1) is expressed as follows $\boldsymbol{w} = \begin{bmatrix} \boldsymbol{P}_d^\top & \boldsymbol{I}_r^\top \end{bmatrix}^\top$ where $\boldsymbol{P}_d$ is the disturbance in load demand and $\boldsymbol{I}_r$ is the disturbance in the sun's irradiance. Furthermore in (1) we model $\boldsymbol{x}_d$ as:

$$\boldsymbol{x}_d(t) := \boldsymbol{x}_d = \begin{bmatrix} \boldsymbol{x}_G^\top & \boldsymbol{x}_R^\top & \boldsymbol{x}_m^\top \end{bmatrix}^\top \tag{3}$$

where $\boldsymbol{x}_G$ denote states of synchronous generators, $\boldsymbol{x}_R$ denote dynamic states of PV plant, and $\boldsymbol{x}_m$ represents dynamic states of motor load. To that end, we model synchronous machines using a comprehensive ninth order generator model, thus $\boldsymbol{x}_G$ can be given as follows [15], [16]:

$$\boldsymbol{x}_G = \begin{bmatrix} \boldsymbol{e}_d^\top & \boldsymbol{e}_q^\top & \boldsymbol{\omega}_{sg}^\top & \boldsymbol{\delta}_{sg}^\top & \boldsymbol{T}_m^\top & \boldsymbol{P}_v^\top & \boldsymbol{E}_{fd}^\top & \boldsymbol{v}_a^\top & \boldsymbol{r}_f^\top \end{bmatrix} \in \mathbb{R}^{9G} \tag{4}$$

where $\boldsymbol{e}_d$, $\boldsymbol{e}_q$ denotes transient voltages along q- and d-axis, $\boldsymbol{\omega}_{sg}$ is the rotor speed, $\boldsymbol{\delta}_G$ is the rotor angle, $\boldsymbol{T}_m$ represents prime mover torque, $\boldsymbol{P}_v$ defines valve position, $\boldsymbol{E}_{fd}$ depicts field voltage, $\boldsymbol{v}_a$ is the amplifier voltage, and $\boldsymbol{r}_f$ denotes stabilizer output [15], [16].

The model for the PV power plant has been obtained from [16] and thus the state vector $\boldsymbol{x}_R$ can be expressed as follows:

$$\boldsymbol{x}_R = \begin{bmatrix} \boldsymbol{i}_{dq_f}^\top & \boldsymbol{v}_{dq_c}^\top & \boldsymbol{E}_{dc}^\top & \boldsymbol{P}_e^\top & \boldsymbol{Q}_e^\top & \boldsymbol{\delta}_{\text{inv}}^\top & \boldsymbol{z}_{dq_0}^\top & \boldsymbol{z}_{dq_f}^\top \end{bmatrix} \in \mathbb{R}^{12J} \tag{5}$$

where $\boldsymbol{i}_{dq_f} = [\boldsymbol{i}_{d_f}^\top \ \boldsymbol{i}_{q_f}^\top]$ denotes the dq-axis current at the terminals of the inverter of the PV plant, $\boldsymbol{v}_{dq_c} = [\boldsymbol{v}_{d_c}^\top \ \boldsymbol{v}_{q_c}^\top]$ is the dq-axis voltage across the AC capacitor, $\boldsymbol{E}_{\text{dc}}$ denotes energy stored in the dc-link capacitor of the PV plant, $\boldsymbol{P}_e$ and

$\boldsymbol{Q}_e$ are the filtered real and reactive power at the terminals of the PV power plant, $\boldsymbol{\delta}_{\text{inv}}$ is the relative angle of the PV power plant, $\boldsymbol{z}_{dq_o}=[\boldsymbol{z}_{d_0}^\top\ \boldsymbol{z}_{q_0}^\top]$ and $\boldsymbol{z}_{dq_f}=[\boldsymbol{z}_{d_f}^\top\ \boldsymbol{z}_{q_f}^\top]$ are the states of the voltage and current regulators used in the grid-forming controller of the PV plant. Readers are referred to [16] for further details and complete in-depth description about the PV power plant model used in this study.

The dynamics of the motor loads are detailed as [17]:

$$\dot{\omega}_{\text{mot}_k} = \frac{1}{2H_{m_k}}(T_{e_k} - T_{m_k}) \tag{6}$$

where H_{m_k} is the motor inertia constant and T_{e_k}, T_{m_k} denotes electromagnetic and mechanical torques in the k-th motor [17, p. 244]. Thus $\boldsymbol{x}_m = [\boldsymbol{w}_{\text{mot}}]$.

To take into account the topological effect of power systems, the power flow/balance or the current balance equations need to considered. These can be expressed as follows [15]:

$$\underbrace{\begin{bmatrix}\widetilde{\boldsymbol{I}}_G\\ \widetilde{\boldsymbol{I}}_R\\ \widetilde{\boldsymbol{I}}_L\end{bmatrix}}_{\boldsymbol{I}} - \underbrace{\begin{bmatrix}\boldsymbol{Y}_{GG} & \boldsymbol{Y}_{GR} & \boldsymbol{Y}_{GL}\\ \boldsymbol{Y}_{RG} & \boldsymbol{Y}_{RR} & \boldsymbol{Y}_{RL}\\ \boldsymbol{Y}_{LG} & \boldsymbol{Y}_{LR} & \boldsymbol{Y}_{LL}\end{bmatrix}}_{\boldsymbol{Y}} \underbrace{\begin{bmatrix}\widetilde{\boldsymbol{V}}_G\\ \widetilde{\boldsymbol{V}}_R\\ \widetilde{\boldsymbol{V}}_L\end{bmatrix}}_{\boldsymbol{V}} = \boldsymbol{0} \tag{7}$$

where $\boldsymbol{I}$ is the net injected current vector, $\boldsymbol{Y}$ is the admittance matrix, and $\boldsymbol{V}$ is the bus voltage vector. In (7), $\widetilde{\boldsymbol{I}}_G = \{I_{Re_i}\}_{i\in\mathcal{G}} + j\{I_{Im_i}\}_{i\in\mathcal{G}}$ denotes phasor currents injected by synchronous generators and $\widetilde{\boldsymbol{V}}_G = \{V_{Re_i}\}_{i\in\mathcal{G}} + j\{V_{Im_i}\}_{i\in\mathcal{G}}$ represents voltage phasors at the terminal of generator buses. Similarly $\widetilde{\boldsymbol{V}}_R$, $\widetilde{\boldsymbol{V}}_L$, $\widetilde{\boldsymbol{I}}_R$, and $\widetilde{\boldsymbol{I}}_L$ denotes voltage and current phasors of all loads and PV power plants.

To that end, by considering (2)–(7) and incorporating the associated dynamics, we can represent the overall SLS-DAE model of a power system in a state-space format:

$$\textbf{SLS-DAE:}\quad \boldsymbol{E}\dot{\boldsymbol{x}} = \boldsymbol{A}\boldsymbol{x} + \boldsymbol{f}(\boldsymbol{x},\boldsymbol{u},\boldsymbol{w}) + \boldsymbol{B}\boldsymbol{u} + \boldsymbol{B}_w\boldsymbol{w} \tag{8a}$$

$$\boldsymbol{y} = \boldsymbol{C}\boldsymbol{x} + \boldsymbol{v} \tag{8b}$$

where $\boldsymbol{x} = \begin{bmatrix}\boldsymbol{x}_d^\top & \boldsymbol{x}_a^\top\end{bmatrix}^\top \in \mathbb{R}^n$ denotes the overall state vector; $\boldsymbol{E}$ encodes algebraic constraints with rows of zeros; $\boldsymbol{C}$ maps state vector $\boldsymbol{x}$ to what PMUs usually measures (i.e., current and voltage phasors) and $\boldsymbol{v} \in \mathbb{R}^p$ denotes measurement noise on PMU measurements $\boldsymbol{y} \in \mathbb{R}^p$. Since vector $\boldsymbol{x}_a$ contains voltage and current phasors, we define $\boldsymbol{C}$ as: $\boldsymbol{C} = \begin{bmatrix}\boldsymbol{O} & \tilde{\boldsymbol{C}}\end{bmatrix}$, where $\tilde{\boldsymbol{C}}$ is a diagonal binary matrix with ones only at those locations where PMUs are connected and voltage and current phasors are measured. The other state-space matrices $\boldsymbol{A}$, $\boldsymbol{B}$ and $\boldsymbol{B}_w$ are obtained by capturing the linear components of the SLS-DAE model. The vector-valued function $\boldsymbol{f}(\cdot)$ captures the encompassed nonlinearities in the dynamics.

III. Estimator for the SLS-DAE Model

In this section, we propose a Luenberger type observer design for the SLS-DAE model depicted in (8). First, we focus on modeling the uncertainties in loads and renewables and present a technique to parameterize the nonlinear function $\boldsymbol{f}(\cdot)$ in the power system dynamics.

A. Modeling uncertainty and bounding nonlinearity

In Eq. (8) the vector $\boldsymbol{w}$ encapsulates load demand and irradiance; both quantities are time-varying and fluctuating. To that end, herein we assume that hour- or minute-ahead predictions of loads and irradiance are available while the fluctuation/disturbances in these quantities are unknown. Notice that this is realistic as power systems operators record and publish these quantities on a daily basis (see daily hour- and minute-ahead predictions of load and renewables published by California independent system operator [18]). However, the prediction may be inaccurate. In particular, high fidelity estimate of RERs are difficult to obtain. Accordingly, we can write $\boldsymbol{w} = \bar{\boldsymbol{w}} + \Delta\boldsymbol{w}$, where $\bar{\boldsymbol{w}}$ is the predicted/known values and $\Delta\boldsymbol{w}$ defines all the disturbances/uncertainties in these quantities. The goal of the estimator is to provide accurate state estimation results under unknown uncertainty $\Delta\boldsymbol{w}$. To that end, the SLS-DAE model (8) can be rewritten as follows:

$$\boldsymbol{E}\dot{\boldsymbol{x}} = \boldsymbol{A}\boldsymbol{x} + \boldsymbol{f}(\boldsymbol{x},\boldsymbol{u},\boldsymbol{w}) + \boldsymbol{B}\boldsymbol{u} + \boldsymbol{B}_w\bar{\boldsymbol{w}} + \boldsymbol{B}_w\Delta\boldsymbol{w} \tag{9a}$$

$$\boldsymbol{y} = \boldsymbol{C}\boldsymbol{x} + \boldsymbol{v}. \tag{9b}$$

To synthesize a robust estimator, it is crucial to identify and parameterize the nonlinearities in the dynamical system. Hence, to express the nonlinear function $\boldsymbol{f}(\cdot)$ in a better way in the SLS-DAE model we assume that $\boldsymbol{f}(\cdot)$ is Lipschitz continuous, which means $\boldsymbol{f}(\cdot)$ is differentiable everywhere and the rate of change is bounded above by a real number. Smallest such real number is called Lipschitz constant. With that in mind we assume $\boldsymbol{x} \in \mathcal{X}$, where $\mathcal{X}$ define the operating region of state vector $\boldsymbol{x}$, then the Lipschitz bounding condition for $\boldsymbol{f}(\cdot)$ can be written as follows:

$$\|\boldsymbol{f}(\boldsymbol{x},\boldsymbol{u},\boldsymbol{w}) - \boldsymbol{f}(\hat{\boldsymbol{x}},\boldsymbol{u},\boldsymbol{w})\|_2 \leq \alpha\|(\boldsymbol{x}-\hat{\boldsymbol{x}})\|_2 \tag{10}$$

where $\alpha \in \mathbb{R}^+$ is the Lipschitz constant. In the case of power systems the Lipschitz constant can be assumed based on operator knowledge and by looking at the overall size/topology of the grid or it can also be computed using much more sophisticated ways as shown in [19], [20]. Also, since the Lipschitz constant provides an operational bound on grid state variables, its value can be varied to consider anomalies and deviations from steady state values and vice versa [2]. Showcasing methods to compute Lipschitz constant is beyond the scope of this paper.

B. H_∞ based state estimator design

In this study we are designing a Luenberger type state estimator for SLS-DAE model of power systems depicted in (9). The overall estimator design is primarily based on Lyapunov stability criterion and H_∞ estimation concept is used to achieve robust performance under unknown fluctuations/disturbances from loads and RERs.

In state estimation literature, the H_∞ concept was proposed in [21] to synthesize a robust estimator for linear systems subject to unknown uncertainty. The main advantage of H_∞ based state estimation is that no prior knowledge or assumptions are required about the statistical properties of

uncertainty. In H_∞ based state estimation the uncertainty is considered as a random bounded signal and then the observer is designed such that it ensures a particular H_∞ performance for the error dynamics for all such bounded uncertainty, such that $\|\boldsymbol{e}\|_{L_2}^2 \leq \gamma^2 \|\Delta \boldsymbol{w}\|_{L_2}^2$ with performance level γ.

That being said, we now focus on presenting the structure of our observer design for the SLS-DAE model of power system depicted in (9). To begin, let $\hat{\boldsymbol{y}}$ be the estimated outputs and $\hat{\boldsymbol{x}}$ be the estimated states variables. Then Luenberger type state estimator for (9) can be expressed as follows:

$$\boldsymbol{E}\dot{\hat{\boldsymbol{x}}} = \boldsymbol{A}\hat{\boldsymbol{x}} + \boldsymbol{f}\left(\hat{\boldsymbol{x}}, \boldsymbol{u}, \bar{\boldsymbol{w}}\right) + \boldsymbol{L}(\boldsymbol{y} - \hat{\boldsymbol{y}}) + \boldsymbol{B}\boldsymbol{u} + \boldsymbol{B}_w \bar{\boldsymbol{w}} \quad (11a)$$

$$\hat{\boldsymbol{y}} = \boldsymbol{C}\hat{\boldsymbol{x}} \quad (11b)$$

where $\boldsymbol{L} \in \mathbb{R}^{n \times p}$ is the estimator gain matrix (a design variable). Even if the estimator starts from different initial conditions, using measurement provided by PMUs $\boldsymbol{y}$, the gain matrix $\boldsymbol{L}$ ensures the convergence of estimated states $\hat{\boldsymbol{x}}$ to their true values $\hat{\boldsymbol{x}}$. The main objective of this study is to design an appropriate gain matrix $\boldsymbol{L}$ such that robust DSE can be achieved from the estimator dynamics (11).

To that end, we define the error between actual and true values of state variables as $\boldsymbol{e} = \boldsymbol{x} - \hat{\boldsymbol{x}}$. Then using (9) and (11) the model for the error dynamics can be computed as:

$$\boldsymbol{E}\dot{\boldsymbol{e}} = \boldsymbol{A}_c \boldsymbol{e} + \Delta \boldsymbol{f} + \boldsymbol{B}_w \Delta \boldsymbol{w} \quad (12)$$

where $\boldsymbol{A}_c = (\boldsymbol{A} - \boldsymbol{L}\boldsymbol{C})$ and $\Delta \boldsymbol{f} = \boldsymbol{f}\left(\boldsymbol{x}, \boldsymbol{u}, \boldsymbol{w}\right) - \boldsymbol{f}\left(\hat{\boldsymbol{x}}, \boldsymbol{u}, \boldsymbol{w}\right)$. The primary objective of the estimator is to drive the DAE of the error (12) near zero under unknown uncertainty $\Delta \boldsymbol{w}$. Before we proceed to the theory of designing the gain matrix $\boldsymbol{L}$, we present key assumption that is critical in developing the proposed methodology.

Assumption 1: The effect of uncertainty $\Delta \boldsymbol{w}$ on the norm of $\boldsymbol{f}(\cdot)$ is negligible, meaning:

$$\|\boldsymbol{f}(\hat{\boldsymbol{x}}, \boldsymbol{u}, \bar{\boldsymbol{w}})\|_2 \approx \|\boldsymbol{f}(\hat{\boldsymbol{x}}, \boldsymbol{u}, \boldsymbol{w})\|_2.$$

Assumption 1 is crucial as it is required while applying the S-procedure lemma [22] in the derivation of estimator gain in a tractable way. Notice that Assumption 1 is mild as the nonlinear function in the power systems models are commonly independent of uncertainties and are mostly dependent only on state vector [15], [23]. To validate this on the SLS-DAE model (11), we test different IEEE test power systems such as WECC 9-bus system and IEEE 39-bus system. We notice that by varying $\boldsymbol{P}_d$ in $\boldsymbol{w}$, the norm of $\boldsymbol{f}(\cdot)$ does not change while by adding uncertainty in $\boldsymbol{I}_r$ the norm of $\boldsymbol{f}(\cdot)$ changes slightly, such as by decreasing the irradiance by 40% the percentage change in $\|\boldsymbol{f}(\cdot)\|_2$ is $0.09 \times 10^{-3}\%$. Hence Assumption 1 is empirically satisfied. Proving Assumption 1 theoretically is an interesting research question beyond the scope of this paper.

We can now find sufficient condition for the existence of observer gain matrix $\boldsymbol{L}$. To that end, we assume a Lyapunov candidate function $V(\boldsymbol{e}) = \boldsymbol{e}^\top \boldsymbol{E}^\top \boldsymbol{P} \boldsymbol{e}$, where $V : \mathbb{R}^n \to \mathbb{R}_+$, $\boldsymbol{P} \in \mathbb{R}^{n \times n}$, and $\boldsymbol{E}^\top \boldsymbol{P} = \boldsymbol{P}^\top \boldsymbol{E} \succeq 0$, then its derivative along the trajectories of (12) yields:

$$\dot{V}(\boldsymbol{e}) = (\boldsymbol{E}\dot{\boldsymbol{e}})^\top \boldsymbol{P}\boldsymbol{e} + (\boldsymbol{P}\boldsymbol{e})^\top (\boldsymbol{E}\dot{\boldsymbol{e}}).$$

For any bounded disturbances $\Delta \boldsymbol{w}$, the H_∞ stability condition can be satisfied as

$$\dot{V}(\boldsymbol{e}) + \boldsymbol{e}^\top \boldsymbol{e} - \gamma^2 \Delta \boldsymbol{w}^\top \Delta \boldsymbol{w} < 0 \quad (13)$$

the above equation can be rearranged as: $\boldsymbol{\Upsilon}^\top \boldsymbol{\Theta}_1 \boldsymbol{\Upsilon} < 0$, where

$$\boldsymbol{\Upsilon} = \begin{bmatrix} \boldsymbol{e} \\ \Delta \boldsymbol{f} \\ \Delta \boldsymbol{w} \end{bmatrix}, \boldsymbol{\Theta}_1 = \begin{bmatrix} \boldsymbol{A}_c^\top \boldsymbol{P} + \boldsymbol{A}_c \boldsymbol{P}^\top + \boldsymbol{I} & \boldsymbol{P}^\top & \boldsymbol{P}^\top \boldsymbol{B}_w \\ \boldsymbol{P} & \boldsymbol{O} & \boldsymbol{O} \\ \boldsymbol{B}_w^\top \boldsymbol{P} & \boldsymbol{O} & -\gamma^2 \boldsymbol{I} \end{bmatrix}.$$

Now from Lipschitz continuity assumption (10) we obtain

$$\Delta \boldsymbol{f}^\top \Delta \boldsymbol{f} - \alpha \boldsymbol{e}^\top \boldsymbol{e} \leq 0 \quad (14)$$

which can be written as $\boldsymbol{\Upsilon}^\top \boldsymbol{\Theta}_2 \boldsymbol{\Upsilon} \leq 0$, with $\boldsymbol{\Theta}_2 = \operatorname{diag}\left(\begin{bmatrix} -\alpha \boldsymbol{I} & \boldsymbol{I} & \boldsymbol{O} \end{bmatrix}\right)$, where diag denotes a diagonal matrix. Now applying the S-procedure Lemma [22], then $\boldsymbol{\Theta}_1 - (\epsilon)\boldsymbol{\Theta}_2 \prec 0$ for some scalar $\epsilon > 0$, which is equivalent to:

$$\begin{bmatrix} \boldsymbol{A}_c^\top \boldsymbol{P} + \boldsymbol{P}^\top \boldsymbol{A}_c + \boldsymbol{I} + \epsilon\alpha \boldsymbol{I} & \boldsymbol{P}^\top & \boldsymbol{P}^\top \boldsymbol{B}_w \\ \boldsymbol{P} & -\epsilon \boldsymbol{I} & \boldsymbol{O} \\ \boldsymbol{B}_w^\top \boldsymbol{P} & \boldsymbol{O} & -\gamma^2 \boldsymbol{I} \end{bmatrix} \prec 0. \quad (15)$$

Now lets suppose there exists two non singular matrices $\boldsymbol{U} \in \mathbb{R}^{n \times n}$ and $\boldsymbol{V} \in \mathbb{R}^{n \times n}$ such that:

$$\boldsymbol{U}^{-\top} \boldsymbol{P} \boldsymbol{V} = \begin{bmatrix} \boldsymbol{P_1} & \boldsymbol{P_2} \\ \boldsymbol{P_3} & \boldsymbol{P_4} \end{bmatrix}, \quad \boldsymbol{U}\boldsymbol{E}\boldsymbol{V} = \begin{bmatrix} \boldsymbol{I} & \boldsymbol{O} \\ \boldsymbol{O} & \boldsymbol{O} \end{bmatrix} \quad (16)$$

where $\boldsymbol{P_1} \in \mathbb{R}^{n_d \times n_d}$, $\boldsymbol{P_2} \in \mathbb{R}^{n_d \times n_a}$, $\boldsymbol{P_3} \in \mathbb{R}^{n_a \times n_d}$ and $\boldsymbol{P_4} \in \mathbb{R}^{n_a \times n_a}$. Then we can write:

$$\boldsymbol{E} = \boldsymbol{U}^{-1} \begin{bmatrix} \boldsymbol{I} & \boldsymbol{O} \\ \boldsymbol{O} & \boldsymbol{O} \end{bmatrix} \boldsymbol{V}^{-1} \quad (17a)$$

$$\boldsymbol{P} = \boldsymbol{U}^\top \begin{bmatrix} \boldsymbol{P_1} & \boldsymbol{P_2} \\ \boldsymbol{P_3} & \boldsymbol{P_4} \end{bmatrix} \boldsymbol{V}^{-1}. \quad (17b)$$

From Eq. (17), $\boldsymbol{P}^\top \boldsymbol{E}$ and $\boldsymbol{E}^\top \boldsymbol{P}$ can be written as:

$$\boldsymbol{E}^\top \boldsymbol{P} = \boldsymbol{V}^{-\top} \begin{bmatrix} \boldsymbol{P_1} & \boldsymbol{O} \\ \boldsymbol{O} & \boldsymbol{O} \end{bmatrix} \boldsymbol{V}^{-1}$$

$$\boldsymbol{P}^\top \boldsymbol{E} = \boldsymbol{V}^{-\top} \begin{bmatrix} \boldsymbol{P_1}^\top & \boldsymbol{O} \\ \boldsymbol{P_2} & \boldsymbol{O} \end{bmatrix} \boldsymbol{V}^{-1}.$$

We need to make $\boldsymbol{P}^\top \boldsymbol{E} = \boldsymbol{E}^\top \boldsymbol{P}$ and it can be done if $\boldsymbol{P_2} = 0$ and $\boldsymbol{P_1} = \boldsymbol{P_1}^\top$. Thus from (16) we can write:

$$\begin{aligned} \boldsymbol{P} &= \boldsymbol{U}^\top \begin{bmatrix} \boldsymbol{P_1} & \boldsymbol{O} \\ \boldsymbol{P_3} & \boldsymbol{P_4} \end{bmatrix} \boldsymbol{V}^{-1} \\ &= \boldsymbol{U}^\top \left(\begin{bmatrix} \boldsymbol{P_1} & \boldsymbol{O} \\ \boldsymbol{O} & \boldsymbol{O} \end{bmatrix} + \begin{bmatrix} \boldsymbol{O} & \boldsymbol{O} \\ \boldsymbol{P_3} & \boldsymbol{P_4} \end{bmatrix} \right) \boldsymbol{V}^{-1} \\ &= \boldsymbol{U}^\top \left(\begin{bmatrix} \boldsymbol{P_1} & \boldsymbol{O} \\ \boldsymbol{O} & \boldsymbol{I} \end{bmatrix} \begin{bmatrix} \boldsymbol{I} & \boldsymbol{O} \\ \boldsymbol{O} & \boldsymbol{O} \end{bmatrix} \right) \boldsymbol{V}^{-1} + \boldsymbol{U}^\top \begin{bmatrix} \boldsymbol{O} & \boldsymbol{O} \\ \boldsymbol{P_3} & \boldsymbol{P_4} \end{bmatrix} \boldsymbol{V}^{-1} \end{aligned}$$

Defining $\boldsymbol{X} \in \mathbb{S}_{++}^{n \times n}$ as:

$$\boldsymbol{X} = \boldsymbol{U}^\top \begin{bmatrix} \boldsymbol{P_1} & \boldsymbol{O} \\ \boldsymbol{O} & \boldsymbol{I} \end{bmatrix} \boldsymbol{U} \quad (19)$$

$$\boldsymbol{P} = \boldsymbol{X}\boldsymbol{E} + \underbrace{\boldsymbol{U}^\top \begin{bmatrix} \boldsymbol{O} \\ \boldsymbol{I} \end{bmatrix}}_{\boldsymbol{E}^{\perp\top}} \underbrace{\begin{bmatrix} \boldsymbol{P_3} & \boldsymbol{P_4} \end{bmatrix} \boldsymbol{V}^{-1}}_{\boldsymbol{Y}} \quad (20a)$$

$$\boldsymbol{P} = \boldsymbol{X}\boldsymbol{E} + \boldsymbol{E}^{\perp\top} \boldsymbol{Y} \quad (20b)$$

where $\boldsymbol{Y} \in \mathbb{R}^{n_a \times n}$ and $\boldsymbol{E}^{\perp\top} \in \mathbb{R}^{n \times n}$ is the orthogonal complement of $\boldsymbol{E}$. Finally, defining $\boldsymbol{N} = \boldsymbol{L}^\top \boldsymbol{P} \in \mathbb{R}^{p \times n}$ and substituting the value of $\boldsymbol{P}$ from (20b) in (15) then the sufficient condition for the existence of observer gain $\boldsymbol{L}$ can be written in term of strict linear matrix inequality (LMI) as follows:

$$\begin{bmatrix} \boldsymbol{\Omega}_{11} & * & * \\ \boldsymbol{E}^{\perp\top}\boldsymbol{Y} + \boldsymbol{X}\boldsymbol{E} & -\epsilon \boldsymbol{I} & * \\ \boldsymbol{B_w}^\top \boldsymbol{X}\boldsymbol{E} + \boldsymbol{B_w}^\top \boldsymbol{E}^{\perp\top}\boldsymbol{Y} & \boldsymbol{O} & -\gamma^2 \boldsymbol{I} \end{bmatrix} \prec 0 \qquad (21)$$

where $\boldsymbol{\Omega}_{11}$ is given as:

$$\boldsymbol{\Omega}_{11} = \boldsymbol{A}^\top \boldsymbol{X}\boldsymbol{E} + \boldsymbol{A}^\top \boldsymbol{E}^{\perp\top}\boldsymbol{Y} + \boldsymbol{E}^\top \boldsymbol{X}^\top \boldsymbol{A} + \boldsymbol{Y}^\top \boldsymbol{E}^\perp \boldsymbol{A} - \boldsymbol{C}^\top \boldsymbol{N} - \boldsymbol{N}^\top \boldsymbol{C} + \epsilon \boldsymbol{\alpha} \boldsymbol{I}.$$

If LMI (21) is solved and there exist matrices $\boldsymbol{N}$, $\boldsymbol{Y}$, $\boldsymbol{X}$, and γ and $\epsilon > 0$, then the estimator gain can be retrieved as $\boldsymbol{L} = \left(\boldsymbol{N}\boldsymbol{P}^{-1}\right)^\top$.

Notice that, since γ denotes performance level, then one can minimize γ to achieve robust performance. Also, minimizing $\|\boldsymbol{N}\|_2$ can provide estimator gain of reasonable magnitude. Furthermore, as our Lyapunov candidate function can be written as $V(\boldsymbol{e}) = \boldsymbol{e}^\top \boldsymbol{E}^\top \boldsymbol{X}\boldsymbol{E}\boldsymbol{e}$ then to achieve quick convergence of $\hat{\boldsymbol{x}}$ to $\boldsymbol{x}$ one can minimize the maximum eigenvalue of $\boldsymbol{E}^\top \boldsymbol{X}\boldsymbol{E}$ which can be written as a convex SDP optimization problem:

$$(\mathbf{P_1}) \quad \underset{\kappa, \boldsymbol{X}}{\text{minimize}} \quad a_3\kappa; \;\; s.t; \;\; \kappa \boldsymbol{I} - \boldsymbol{E}^\top \boldsymbol{X}\boldsymbol{E} \succ 0, \kappa > 0.$$

Hence, the sufficient condition of computing $\boldsymbol{L}$ given in Eq. (21) can be converted to a convex semidefinite optimization problem expressed as follows:

$$\begin{aligned} (\mathbf{P_2}) \quad \underset{\kappa,\epsilon,\gamma,\boldsymbol{N},\boldsymbol{X},\boldsymbol{Y}}{\text{minimize}} \quad & a_1\|\boldsymbol{N}\|_2 + a_2\gamma + a_3\kappa \\ \text{subject to} \quad & \kappa \boldsymbol{I} - \boldsymbol{E}^\top \boldsymbol{X}\boldsymbol{E} \succ 0, \text{LMI (21)}, \\ & \boldsymbol{X} \succ 0, \kappa > 0, \; \epsilon > 0, \gamma > 0 \end{aligned}$$

where a_1, a_2, $a_3 \in \mathbb{R}_{++}$ are predefined weighting constants. Calculating estimator gain matrix $\boldsymbol{L}$ by solving $\mathbf{P_2}$ ensures that the performance of state error dynamics (12) is bounded in the H_∞ sense, such that $\|\boldsymbol{e}\|_{L_2}^2 \leq \gamma^2 \|\Delta \boldsymbol{w}\|_{L_2}^2$. In other words, solving $\mathbf{P_2}$ guarantees that $\|\boldsymbol{e}\|_{L_2}^2$ always lies in a tube of radius $\gamma^2\|\boldsymbol{w}\|_{L_2}^2$. In the next section we present case studies to assess the performance of the estimator.

IV. System Setup and Case Studies

The proposed estimator has been tested on modified IEEE 39-bus system [24]. This system consists of two PV power plants at Buses 34 and 36, a motor load at Bus 14, eight synchronous generators, constant power loads and constant impedance loads. The one-line diagram of this system is depicted in Fig. 1. All the parameters for the synchronous generator and its excitation systems are detailed in [15], while the parameters of PV power plants and a complete in-depth description of the system can be found in [16]. To ensure observability of the test power system we follow the literature and deploy optimal number of PMUs on buses $[2, 6, 9, 10, 13, 14, 17, 19, 20, 22, 23, 25, 29]$ as given in [25]. Each PMU at a bus is measuring the total current demanded/injected and voltage phasors of that bus. The dynamic states that we are estimating are $\boldsymbol{x}_a$ and $\boldsymbol{x}_d$ as given in (2) and (3). The uncertain quantities for the estimator are assumed to be the overall load demand and irradiance from the sun. Moreover, for all the case studies Gaussian noise with diagonal covariance matrix and variance of 0.001^2 has also been added to the PMU measurements.

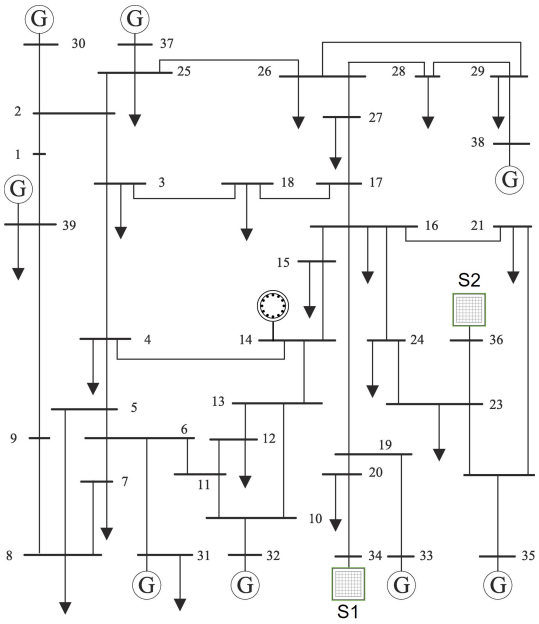

Fig. 1. IEEE 39-bus system with two PV Power Plants at Buses 34, 36 and a motor load at Bus 14.

Both the estimator and power system SLS-DAE models are simulated using MATLAB differential algebraic equations solver `ode15s`, whereas the SDP optimization problem $\mathbf{P_2}$ is solved in YALMIP [26] with MOSEK [27] as optimization solver. The initial conditions for the power system are computed using power flow solutions, while the estimator is initialized from random initial conditions having 10% variation from the steady state values of power system.

A. Case 1: Estimation under demand disturbance

In power systems the overall load demand is usually fluctuating and the exact estimate of the load demand of any power network is difficult to predict. To that end, herein we demonstrate the performance of the proposed estimator in performing DSE under unknown disturbances in power demand. To showcase the robustness of the estimator we provide only steady state values of loads to the estimator and the actual transient/fluctuating values are kept unknown. To generate random fluctuations in the constant power loads we provide step disturbances at $t = 3$s to the loads connected at Buses $[7, 8, 12, 14, 15, 16, 18, 20]$, while the loads connected at Buses 3 and 4 are assumed to be changing sinusoidally with some Gaussian noise as shown in Fig. 3.

The estimation results for the PV Power Plant 1 are shown in Fig 2. We notice that although the estimator starts from initial conditions different than system steady state values

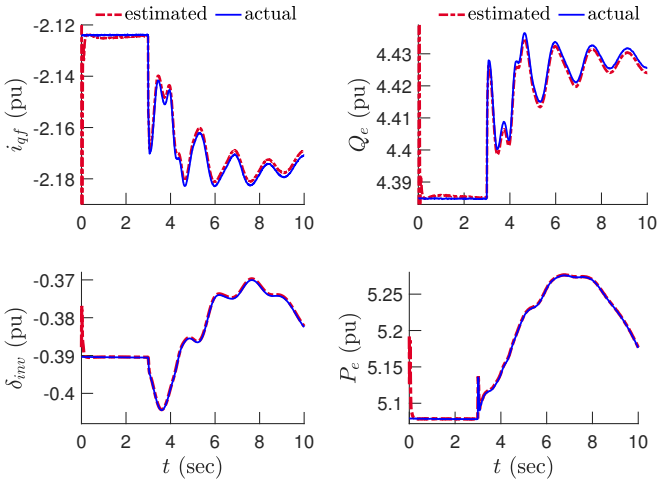

Fig. 2. State estimation results for PV Power Plant 1 under disturbances in real power demand.

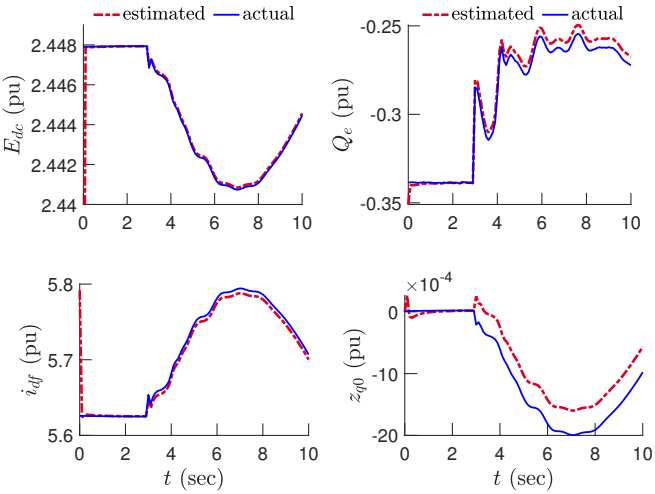

Fig. 4. State estimation results for PV Power Plant 2 under disturbances in real power demand.

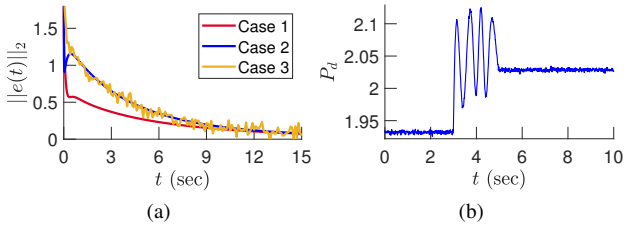

Fig. 3. (a) Estimation error norm for all the case studies (b) Unknown variation in real power demand at Buses 3 and 4.

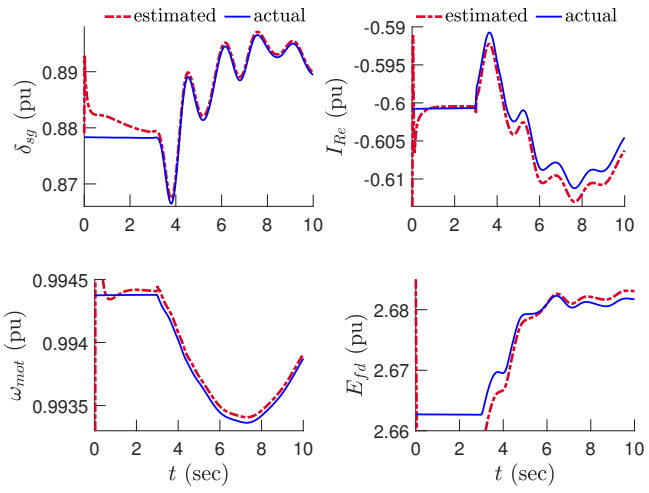

Fig. 5. Estimation results for Generator 6, real current at Bus 21, and motor speed under disturbance in real power demand.

and after $t = 3$s the fluctuations in load demand are not known to the estimator, it can still accurately track the different states of the PV power plant. This can also be corroborated from the estimation error norm given in Fig. 3 from which we can validate that the estimator is successfully driving the error between true and estimated values near zero for all of the system dynamic and algebraic states, under uncertainty. Similar performance from the estimator has been achieved in predicting the dynamic states of PV Power Plant 2, internal states of the synchronous machines, and algebraic variables of all the buses as shown in Figs. 4 and 5.

B. Case 2: Estimation under irradiance and reactive power uncertainty

To further assess the robustness of the estimator toward different sources of uncertainty, in this section we demonstrate the performance of the estimator under disturbances from renewables. To that end, right after $t > 0$ we decreased the irradiance from the sun on both of the PV power plants by 20%. Also, to create further unknown transient conditions we added step disturbances in the overall reactive power demand of the system. Note that, the estimator is completely unaware of these disturbances and only knows the steady state value of these quantities. This can be validated from the structure of the proposed estimator design (11). We can see that the estimator only has access to $\bar{\boldsymbol{w}}$ which contains the steady state/predicted values of load demand and irradiance.

The estimation results for the dynamic state of motor load and Generator 1 are depicted in Fig. 6. We can see that after starting from different initial conditions the observer can successfully converge to the true values of the states variables. Similarly the estimation results for PV Power Plant 1 and algebraic states of Bus 7 are presented in Figs. 7 and 8. We can see that although PMU sensors are not deployed at these buses, the proposed observer can accurately track the true values of state variables. This can also be validated from the estimation error norm given in Fig. 3, we can see that the observer is successfully driving the error norm near zero.

C. Case 3: Estimation under high level of noise from PMU sensors

In this section we briefly assess the robustness of the estimator under higher noise levels from PMU sensors. To that end, we add Gaussian noise with a diagonal covariance

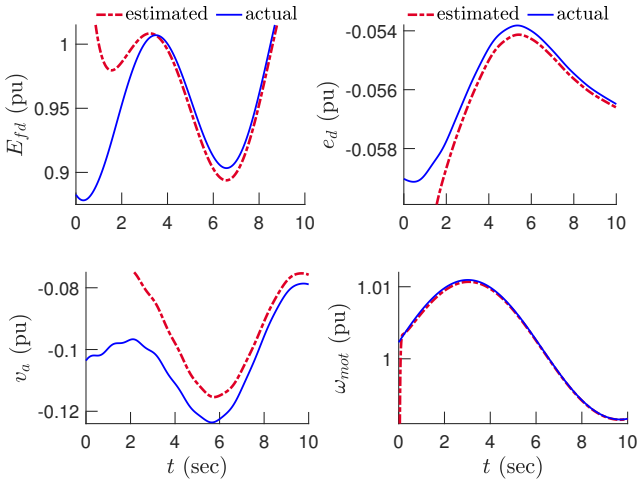

Fig. 6. Estimation results for Case 2: Internal states of Generator 1 and motor speed.

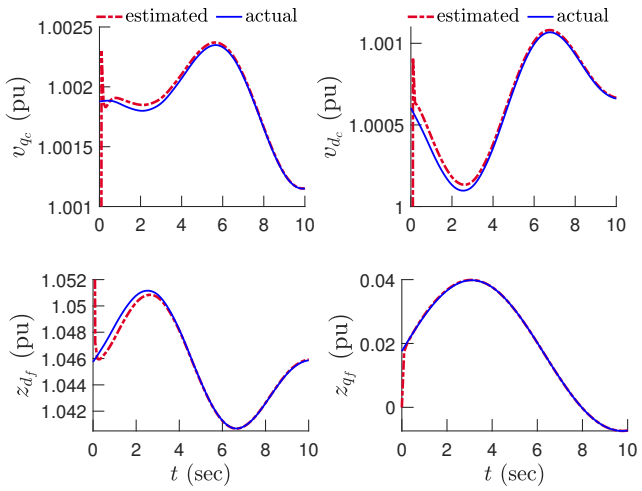

Fig. 7. Estimation results for PV power plant 1 under irradiance and reactive power disturbances.

matrix and having variance 0.01 to the PMU measurements. The estimation results are shown in Figs. 9 and 10. We can see that the observer can still provide good estimation results and is also driving the error norm near zero as shown in Fig. 3. We also notice that with a high level of noise in the PMU measurements, although the estimated states converge to their true values, the quality of state estimation gets poorer. This is because in H_∞ based observer design as discussed in Section III, the observer tries to keep the norm of the estimation error norm less then a constant times the norm of the uncertainty, such that $\|\boldsymbol{e}\|_{L_2}^2 \leq \gamma^2 \|\Delta \boldsymbol{w}\|_{L_2}^2$. Now if the magnitude/level of the uncertainty is higher, then H_∞ condition may not be strict enough and thus providing more room for the observer to give poor estimation results [28]–[30]. Hence in H_∞ based observer design although the observer does not require any statistical properties of the disturbances/uncertainty, the uncertainty should be bounded and its magnitude should be

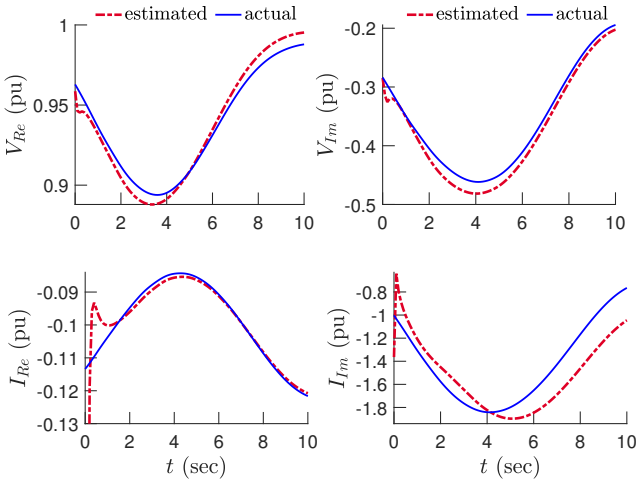

Fig. 8. Estimation results for the complex voltage and current of Bus 7 under irradiance and reactive power disturbances.

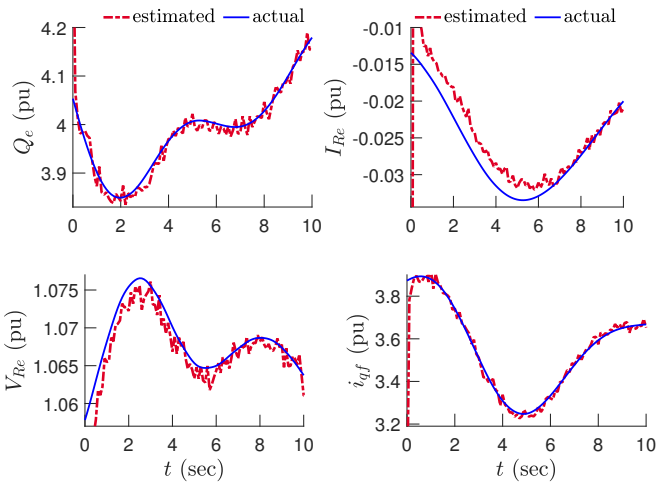

Fig. 9. Estimation results for Case 3 with higher PMU noise of PV Power Plant 2 and algebraic variables of Bus 11.

smaller for the observer to provide accurate results.

V. Summary and Future Work

In this paper, we present a robust estimator for solar and load integrated model of power systems. The observer design is posed as a convex optimization and works as a one step predictor. Using a few measurements provided by PMUs the proposed estimator can provide accurate estimates of all the states of a power system including dynamic states of PV power plants, motor loads, and algebraic states of all buses. The presented estimator does not require any prior knowledge about the statistical properties of the uncertainty and can provide accurate estimation results as long as the uncertainty/disturbance is bounded.

The limitations of this study are twofold: First, the proposed estimator performs DSE in a centralized fashion, thus for a very big power network it needs to be extended to a decentralized framework. Second, the theory of the proposed estimator is based on continuous models, however PMUs

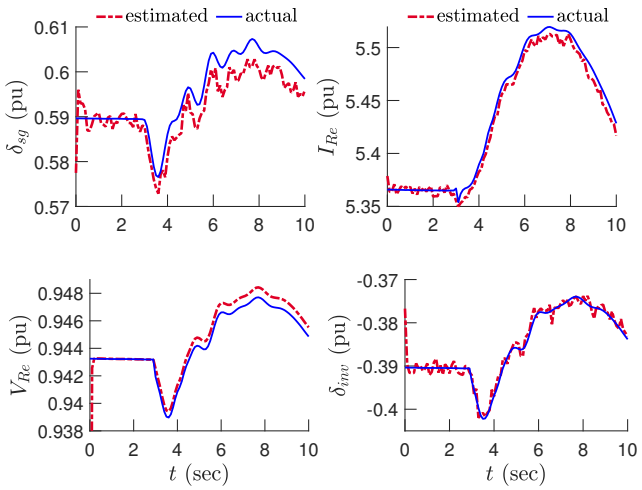

Fig. 10. Estimation results for Case 3 with high level of noise in the PMU sensors: PV power 1, Generator 3, and algebraic variables of 5.

measurements are commonly transmitted via a digitized network, thus a discrete time version of this estimator will be more appropriate. To that end, as a future work the proposed estimator will be extended to a discretized and decentralized framework.

VI. Acknowledgments

The power system model used in this study was developed by Dr. Hugo Villegas Pico (hvillega@iastate.edu) and Soummya Roy (soummyar@iastate.edu) at Iowa State University with support of the National Science Foundation Grants 2013739 and 2151571.

References

[1] Y. Liu, A. K. Singh, J. Zhao, A. P. S. Meliopoulos, B. C. Pal, M. A. Bin Mohd Ariff, T. Van Cutsem, M. Glavic, Z. Huang, I. Kamwa, L. Mili, A. S. Mir, A. F. Taha, V. Terziya, and S. Yu, "Dynamic state estimation for power system control and protection," *IEEE Transactions on Power Systems*, pp. 1–1, 2021.

[2] S. A. Nugroho, A. F. Taha, and J. Qi, "Robust dynamic state estimation of synchronous machines with asymptotic state estimation error performance guarantees," *IEEE Transactions on Power Systems*, vol. 35, no. 3, pp. 1923–1935, 2020.

[3] S. A. Nugroho, A. Taha, N. Gatsis, and J. Zhao, "Observers for differential algebraic equation models of power networks: Jointly estimating dynamic and algebraic states," *IEEE Transactions on Control of Network Systems*, pp. 1–1, 2022.

[4] S. Wang, R. Huang, Z. Huang, and R. Fan, "A robust dynamic state estimation approach against model errors caused by load changes," *IEEE Transactions on Power Systems*, vol. 35, no. 6, pp. 4518–4527, 2020.

[5] M. Jin, H. Feng, and J. Lavaei, "Multiplier-based observer design for large-scale lipschitz systems," 2018.

[6] C. E. A. F. Chiara Mellucci, Prathyush P Menon, "Second-order sliding mode observers for fault reconstruction in power networks," *IET Control Theory and Applications*, vol. 35, no. 6, pp. 4518–4527, 2017.

[7] Z. Huang, K. Schneider, and J. Nieplocha, "Feasibility studies of applying kalman filter techniques to power system dynamic state estimation," in *2007 International Power Engineering Conference (IPEC 2007)*, 2007, pp. 376–382.

[8] E. Ghahremani and I. Kamwa, "Local and wide-area pmu-based decentralized dynamic state estimation in multi-machine power systems," *IEEE Transactions on Power Systems*, vol. 31, no. 1, pp. 547–562, 2016.

[9] J. Zhao, "Dynamic state estimation with model uncertainties using $\mathcal{H}_\infty$ extended kalman filter," *IEEE Transactions on Power Systems*, vol. 33, no. 1, pp. 1099–1100, 2018.

[10] A. K. Singh and B. C. Pal, "Decentralized dynamic state estimation in power systems using unscented transformation," *IEEE Transactions on Power Systems*, vol. 29, no. 2, pp. 794–804, 2014.

[11] N. Zhou, D. Meng, and S. Lu, "Estimation of the dynamic states of synchronous machines using an extended particle filter," *IEEE Transactions on Power Systems*, vol. 28, no. 4, pp. 4152–4161, 2013.

[12] N. Zhou, D. Meng, Z. Huang, and G. Welch, "Dynamic state estimation of a synchronous machine using pmu data: A comparative study," *IEEE Transactions on Smart Grid*, vol. 6, no. 1, pp. 450–460, 2015.

[13] J. Qi, A. F. Taha, and J. Wang, "Comparing kalman filters and observers for power system dynamic state estimation with model uncertainty and malicious cyber attacks," *IEEE Access*, vol. 6, pp. 77 155–77 168, 2018.

[14] Z. Fang, Y. Lin, S. Song, C. Li, X. Lin, and Y. Chen, "State estimation for situational awareness of active distribution system with photovoltaic power plants," *IEEE Transactions on Smart Grid*, vol. 12, no. 1, pp. 239–250, 2021.

[15] P. Sauer, M. Pai, and J. Chow, *Power System Dynamics and Stability: With Synchrophasor Measurement and Power System Toolbox*, ser. Wiley - IEEE. Wiley, 2017.

[16] H. N. V. Pico and B. B. Johnson, "Transient stability assessment of multi-machine multi-converter power systems," *IEEE Transactions on Power Systems*, vol. 34, no. 5, pp. 3504–3514, 2019.

[17] P. C. Krause, O. Wasynczuk, S. D. Sudhoff, and S. D. Pekarek, *Analysis of Electric Machinery and Drive Systems*, 3rd ed. John Wiley & Sons, 2013.

[18] CAISO, "Real time demand curves," Nov 2021. [Online]. Available: http://www.caiso.com/outlook/SystemStatus.html

[19] S. A. Nugroho, A. F. Taha, and J. Qi, "Characterizing the nonlinearity of power system generator models," in *2019 American Control Conference (ACC)*, 2019, pp. 1936–1941.

[20] S. A. Nugroho, A. Taha, and V. Hoang, "Nonlinear dynamic systems parameterization using interval-based global optimization: Computing lipschitz constants and beyond," *IEEE Transactions on Automatic Control*, pp. 1–1, 2021.

[21] U. Shaked, "$\mathcal{H}_\infty$ minimum error state estimation of linear stationary processes," *IEEE Transactions on Automatic Control*, vol. 35, no. 5, pp. 554–558, 1990.

[22] P. M. C. Derinkuyu, Kurşad, "On the s-procedure and some variants," *Mathematical Methods of Operations Research*, vol. 64, no. 1, pp. 55–77, 2016.

[23] S. A. Nugroho and A. F. Taha, "Load and renewable-following control of linearization-free differential algebraic equation power system models," 2021. [Online]. Available: https://arxiv.org/abs/2104.05957

[24] I. Hiskens, *IEEE PES task force on benchmark systems for stability controls*. IEEE PES, Piscataway, NJ, USA, Tech. Rep., IEEE PES, Piscataway, NJ, USA, Tech. Rep, Nov. 2013.

[25] S. Chakrabarti and E. Kyriakides, "Optimal placement of phasor measurement units for power system observability," *IEEE Transactions on Power Systems*, vol. 23, no. 3, pp. 1433–1440, 2008.

[26] J. Lofberg, "Yalmip : a toolbox for modeling and optimization in matlab," in *2004 IEEE International Conference on Robotics and Automation (IEEE Cat. No.04CH37508)*, 2004, pp. 284–289.

[27] E. D. Andersen and K. D. Andersen, *The Mosek Interior Point Optimizer for Linear Programming: An Implementation of the Homogeneous Algorithm*. Boston, MA: Springer US, 2000, pp. 197–232.

[28] A. Zemouche and M. Boutayeb, "Nonlinear-observer-based $\mathcal{H}_\infty$ synchronization and unknown input recovery," *IEEE Transactions on Circuits and Systems I: Regular Papers*, vol. 56, no. 8, pp. 1720–1731, 2009.

[29] A. Thabet, G. B. H. Frej, and M. Boutayeb, "Observer-based feedback stabilization for lipschitz nonlinear systems with extension to $\mathcal{H}_\infty$ performance analysis: Design and experimental results," *IEEE Transactions on Control Systems Technology*, vol. 26, no. 1, pp. 321–328, 2018.

[30] T.-P. Pham, O. Sename, and L. Dugard, "Unified $\mathcal{H}_\infty$ observer for a class of nonlinear lipschitz systems: Application to a real er automotive suspension," *IEEE Control Systems Letters*, vol. 3, no. 4, pp. 817–822, 2019.